Applied Catalysis B: Environmental 187 (2016) 163–170

Contents lists available at ScienceDirect

Applied Catalysis B: Environmental

journal homepage: www.elsevier.com/locate/apcatb

Enhanced photocatalytic activity and photoinduced stability of Ag-based photocatalysts: The synergistic action of amorphous-Ti(IV) and Fe(III) cocatalysts

Huogen Yu[a,b,*], Wuying Chen[a], Xuefei Wang[a], Ying Xu[a], Jiaguo Yu[c]

[a] School of Chemistry, Chemical Engineering and Life Sciences, Wuhan University of Technology, Wuhan 430070, People's Republic of China
[b] State Key Laboratory of Silicate Materials for Architectures, Wuhan University of Technology, Wuhan 430070, People's Republic of China
[c] State Key Laboratory of Advanced Technology for Material Synthesis and Processing, Wuhan University of Technology, Wuhan 430070, People's Republic of China

ARTICLE INFO

Article history:
Received 22 October 2015
Received in revised form
31 December 2015
Accepted 9 January 2016
Available online 13 January 2016

Keywords:
Photocatalyst
Cocatalyst modification
Synergistic action
Photoinduced stability
Amorphous Ti(IV)

ABSTRACT

In recent years, Ag-based materials have attracted a great deal of attentions due to their excellent photocatalytic performance. However, the rapid recombination of photogenerated charges and the poor photostability cause an obvious decrease of their photocatalytic performance. In this study, amorphous Ti(IV) as a hole cocatalyst was first successfully loaded on the surface of AgBr photocatalyst by a facile impregnation method. It was found that the photocatalytic activity of AgBr could be greatly improved by a factor of 1.5 when the loading amount of Ti(IV) cocatalyst was 0.05 wt%. Moreover, in addition to the AgBr, the amorphous Ti(IV) could also be used as an effective hole cocatalyst to greatly improve the photocatalytic performance of other Ag-based materials (such as AgCl, AgI, Ag_2O, Ag_2CO_3, and Ag_3PO_4). However, owing to the rapid transfer of photogenerated holes by Ti(IV) cocatalyst, more photogenerated electrons were accumulated on the conduction band of AgBr, causing an obvious deactivation due to the reduction of surface lattice Ag^+ ions to metallic Ag. In this case, after the further surface modification by Fe(III) as an electron cocatalyst, the photoinduced stability and photocatalytic activity of Ti(IV)/AgBr could be significantly enhanced. The possible reason is due to the synergistic action of amorphous Ti(IV) and Fe(III) cocatalysts, namely, Ti(IV) cocatalyst acts as a hole-capture center to efficiently transfer holes to oxidize organic contaminants, while Fe(III) cocatalyst functions as a reduction active site to reduce oxygen efficiently. Compared with the expensive noble metal cocatalyst (such as Au, Pt, and RuO_2), the surface modification by low-cost transition metal cocatalysts (such as Ti and Fe) is a significant method to develop highly efficient photocatalytic materials.

1. Introduction

Photocatalysis technology plays a crucial role in the treatments of wastewater and air pollution owing to its strong oxidizing ability and environmentally friendly property [1–6]. In recent years, Ag-based compounds as the typical visible-light-driven photocatalysts have received growing attentions, and various Ag-based materials such as AgCl [7–10], AgBr [11–13], AgI [14,15], Ag_3PO_4 [16–19] and Ag_2O [20,21] have been widely reported. Compared with the typical visible-light N-TiO_2 photocatalyst, the Ag-based photocatalysts usually show a higher photocatalytic performance for the degradation of various organic contaminants [22,23]. However, the rapid recombination rate of photogenerated electron-hole pairs in the photocatalysts results in a low photocatalytic efficiency. Therefore, to further enhance the photocatalytic performance of Ag-based photocatalysts, abundant strategies have been performed, such as morphology modulation [24,25], composite materials [26,27], and cocatalyst modification [12,28]. Among these reported methods, cocatalyst modification has been demonstrated to be one of the most important strategies to enhance the photocatalytic performance of various materials by effectively separating photogenerated charges. More importantly, only a small amount of cocatalyst can drastically increase the photocatalytic activity by some simple synthetic strategies [12,17,28].

For the efficient photocatalytic degradation of organic contaminants, the rapid transfer of photogenerated holes onto the

* Corresponding author at: School of Chemistry, Chemical Engineering and Life Sciences, Wuhan University of Technology, Wuhan 430070, People's Republic of China.
E-mail address: yuhuogen@whut.edu.cn (H. Yu).

http://dx.doi.org/10.1016/j.apcatb.2016.01.011
0926-3373/

photocatalyst surface and their following effective oxidation for organic substances are highly required. As a consequence, the surface modification by loading hole cocatalyst is an efficient route to improve the photocatalytic performance via the rapid capture of interfacial holes and promoting their rapid oxidization reaction. At present, the well-known hole cocatalysts such as RuO_2 [29], IrO_2 [30] and PdS [31] have been widely investigated and applied in photocatalytic reactions. However, the above reported noble metals are usually expensive and scarce, thus largely limiting their practical applications. Hence, it is necessary and important to develop some nontoxic and economical hole-cocatalyst materials. In fact, some low-cost hole cocatalysts such as CoO_x [32], Fe_2O_3 [33] and $B_2O_{3-x}N_x$ [34] have been developed and applied in various photocatalytic systems. Recently, amorphous TiO_2 (Ti(IV)) was also found to show excellent ability to capture photogenerated holes. For example, Liu et al. have demonstrated that amorphous Ti(IV) can work as a hole-trapping center on the surface of rutile TiO_2 to effectively decompose organic pollutants [35]. In addition, the amorphous TiO_2 film has also been reported to be a very good carrier of photogenerated holes on semiconductor photoelectrodes such as $BiVO_4$ and GaAs [36,37]. However, the relevant reports about amorphous Ti(IV) as the hole cocatalyst are still very limited. In view of its nontoxic, low-cost and abundant in natural resources, it is very meaningful and interesting to investigate whether amorphous Ti(IV) can act as a general cocatalyst to improve the photocatalytic performance of other photocatalysts.

In this paper, we successfully modified Ag-based materials (such as AgCl, AgBr, AgI, Ag_2O, Ag_2CO_3, and Ag_3PO_4) with amorphous Ti(IV) as the hole cocatalyst by a simple impregnation method. After the Ti(IV) modification, all the resultant Ti(IV)/Ag-based photocatalysts exhibited an obviously enhanced photocatalytic performance for the photodegradation of phenol, suggesting that amorphous Ti(IV) can be used as a general hole cocatalyst to greatly improve the photocatalytic performance of various Ag-based materials. However, owing to the rapid transfer and capture of photogenerated holes by Ti(IV) cocatalyst, more photogenerated electrons were accumulated on the conduction band (CB) of AgBr, causing an obvious deactivation due to the reduction of surface lattice Ag^+ ions to metal Ag. To prevent the deactivation (the rapid reduction of lattice Ag^+ ions) in Ti(IV)/AgBr and to improve its photoinduced stability, the well-known Fe(III) electron-cocatalyst was further loaded on its surface to prepare the Fe(III)-Ti(IV)/AgBr photocatalyst. In this case, it is expected that the Fe(III) electron-cocatalyst can inhibit the deactivation progress of Ti(IV)/Ag-based photocatalysts and improve their photoinduced stability by rapidly trapping excess photogenerated electrons. In fact, it was found that both the photocatalytic activity and photostability of Ti(IV)/Ag-based photocatalysts could be significantly enhanced by loading Fe(III) cocatalyst. To the best of our knowledge, this is the first report about the enhanced photocatalytic activity and photostability of Ag-based photocatalysts by the simultaneous modification of amorphous Ti(IV) and Fe(III) cocatalysts. This work may open a new sight for the development of low-cost and highly efficient photocatalytic materials.

2. Experimental

2.1. Preparation of AgBr photocatalyst

In a typical synthesis of AgBr photocatalyst, 50 mL of $AgNO_3$ solution (0.01 mol L^{-1}) was dropped into 50 mL of NaBr solution (0.01 mol L^{-1}) under magnetic stirring at room temperature. Then the mixture was continuously stirring for another 30 min to obtain a yellow suspension. The resulting suspension was maintained at 60 °C for 2 h. Finally, the precipitate was harvested by filtration, rinsed with distilled water, and dried at room temperature.

To obtain the Ag/AgBr composite, the as-obtained AgBr photocatalyst was dispersed into 10 mL of MO solution (20 mg L^{-1}) and then irradiated using a Xe lamp ($\lambda > 400$nm, 40 mW cm^{-2}) for 30 min. During light irradiation, the color of AgBr powder changed gradually from yellow to gray, implying the formation of Ag nanoparticles. To simply the sample name, the resultant Ag/AgBr was referred to as AgBr (Fig. 1a).

2.2. Preparation of Ti(IV)/AgBr photocatalyst

Ti(IV)/AgBr photocatalysts were prepared by an impregnation method (Fig. 1c). In short, 0.1 g of AgBr was uniformly dispersed into 10 mL of distilled water under constant magnetic stirring. Then a known amount of $Ti(SO_4)_2$ solution (5 mol L^{-1}) was injected into the above suspension quickly. After stirring for 30 min, the above mixture was maintained at 80 °C for 1 h. In this case, the hydrolysis of $Ti(SO_4)_2$ would occur to produce amorphous TiO_2 on the surface of AgBr due to a low temperature. To investigate the effect of Ti(IV)-cocatalyst content on the microstructures and photocatalytic performance of AgBr photocatalyst, the amount of Ti(IV) cocatalyst was controlled to be 0, 0.01, 0.05, 0.1, 0.5 and 1 wt%, and the resultant Ti(IV)/AgBr samples were referred to as AgBr, Ti(IV)/AgBr (0.01 wt%), Ti(IV)/AgBr (0.05 wt%), Ti(IV)/AgBr (0.1 wt%), Ti(IV)/AgBr (0.5 wt%), Ti(IV)/AgBr (1 wt%), respectively. To simply the sample name, the resultant samples were referred to as Ti(IV)/AgBr (X) (X = 0.01, 0.05,0.1, 0.5 and 1 wt%).

2.3. Preparation of other Ti(IV)/Ag-based photocatalysts

The preparation of other Ti(IV)/Ag-based composites (AgCl, AgI, Ag_2O, Ag_2CO_3, and Ag_3PO_4) was similar to that of Ti(IV)/AgBr photocatalyst. Typically, $AgNO_3$ solution was dropped into NaCl, KI, NaOH, K_2CO_3, and Na_2HPO_4 solutions under magnetic stirring to prepare the above Ag-based photocatalysts, respectively. For the loading of Ti(IV) on the various Ag-based photocatalysts, the content of Ti(IV) cocatalyst was controlled to be 0.05 wt%, and the resultant products were referred to as Ti(IV)/AgCl (0.05 wt%), Ti(IV)/AgI (0.05 wt%), Ti(IV)/Ag_2O (0.05 wt%), Ti(IV)/Ag_2CO_3 (0.05 wt%), and Ti(IV)/Ag_3PO_4 (0.05 wt%), respectively.

2.4. Preparation of Fe(III)–Ti(IV)/AgBr photocatalyst

The Fe(III)–Ti(IV)/AgBr photocatalyst was prepared by a simple impregnation method (Fig. 1d). Firstly, the Ti(IV)/AgBr (0.05 wt%) photocatalyst was synthesized under an identical experimental condition as described in Section 2.2. Then, 0.1 g of the as-obtained Ti(IV)/AgBr photocatalyst was dispersed into 10 mL of $Fe(NO_3)_3$ aqueous solution (0.01 mol L^{-1}) under constant stirring. After stirring at 60 °C for 2 h, the resulting sample was collected by filtration, washed by deionized water, and dried at 60 °C to obtain Fe(III)–Ti(IV)/AgBr (0.05 wt%) photocatalyst. For comparison, we also prepared Fe(III)-modified AgBr photocatalyst (Fe(III)/AgBr) by the same method (Fig. 1b).

2.5. Characterization

The field emission scanning electron microscope (FESEM) measurements were implemented by using a Hitachi JEM-7500F system. X-ray diffraction (XRD) measurements were carried out on a D/MAX-RB X-ray diffractometer (Rigaku, Japan). X-ray photoelectron spectroscopy (XPS) was obtained on an KRATOA XSAM800 XPS system with Mg Kα source. The binding energies were referenced to the C1s line at 284.8 eV from adventitious carbon. UV–vis

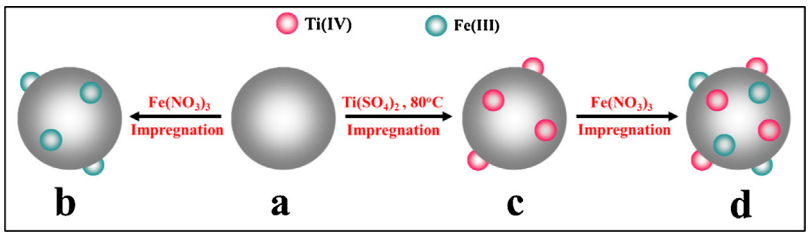

Fig. 1. Schematic diagram illustrating the controllable preparation of various samples: (a) AgBr; (b) Fe(III)/AgBr; (c) Ti(IV)/AgBr (0.05 wt%); and (d) Fe(III)–Ti(IV)/AgBr (0.05 wt%).

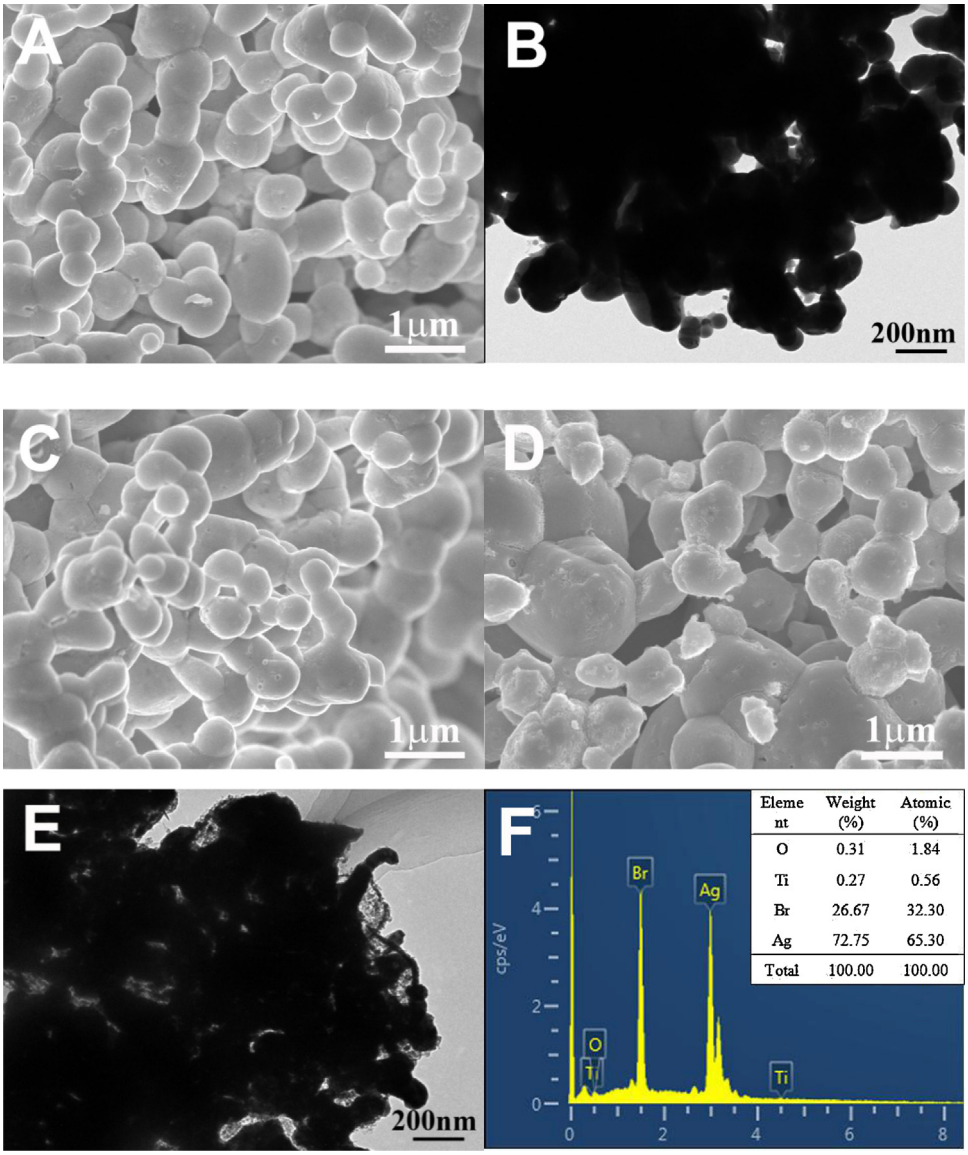

Element	Weight (%)	Atomic (%)
O	0.31	1.84
Ti	0.27	0.56
Br	26.67	32.30
Ag	72.75	65.30
Total	100.00	100.00

Fig. 2. (A,C,D) FESEM and (B,E) TEM images of various samples: (A,B) AgBr; (C) Ti(IV)/AgBr (0.05 wt%); (D,E) Ti(IV)/AgBr (0.5 wt%); and (F) EDS of Ti(IV)/AgBr (0.5 wt%).

absorption spectra were obtained on a UV–vis spectrophotometer (UV-2450, Shimadzu, Japan). $BaSO_4$ was used as a reflectance standard in a UV–vis diffuse reflectance experiment.

2.6. Photocatalytic activity

The photocatalytic performance of the resulting samples was evaluated by photodegradation of phenol aqueous solution at ambient temperature. Experimental details were shown as follows: 70 mg of the photocatalyst was dispersed into 10 mL of phenol solution (20 mg L^{-1}) in a disk with a diameter of ca. 5 cm. Before irradiation, the suspension was placed in the dark for 30 min to achieve an adsorption-desorption equilibrium. Two 5-W 420-nm LED lights were used as the visible-light sources. At a given interval, the concentration of phenol solution was detected on a UV–vis spectrophotometer (UV-1240, SHIMADZU, Japan). In view of a low concentration of the phenol solution, its photodegradation progress is a pseudo-first-order reaction and its kinetics may be expressed

as $\ln(c_0/c) = kt$, where k represents the apparent rate constant, c_0 represents the original concentration of phenol solution, and c represents the concentration of phenol solution after irradiation for t min [17,28].

3. Results and discussion

3.1. Morphology and microstructures of Ti(IV)/AgBr photocatalyst

The FESEM and TME images of the as-prepared samples are shown in Fig. 2. It can be seen that the size of AgBr (Fig. 2A and B) is in the range of 0.2–1 μm due to a simple precipitation method, and the particle surface is smooth. The corresponding XRD pattern (Fig. 3a) clearly suggests the formation of AgBr phase (JCPDS no. 06-0438). After loading Ti(IV) cocatalyst (0.05 wt%) on its surface (Fig. 2C), the particle morphology and size show no obvious difference compared with the pure AgBr (Fig. 2A). In view of a low amount of Ti(IV) cocatalyst, no related diffraction peaks belonging to Ti(IV) compounds can be detected (Fig. 3b). When the amount of Ti(IV) increases to 0.5 wt%, the AgBr particles show a relatively rough surface and some small nanoparticles can clearly be observed (Fig. 2D). The TEM image (Fig. 2E) also obviously suggests the formation of many nanoparticles with a size of less than 10 nm on the AgBr surface, although no additional diffraction peaks can be observed (Fig. 3c). To investigate the components of those small particles in Ti(IV)/AgBr (0.5 wt%), the EDS analysis is performed and its corresponding result is shown in Fig. 2F. It is found that in addition to the main Ag and Br elements, the Ti and O elements can also be observed and the atom ratio of Ti to O is ca. 1:3.3, a value lower than

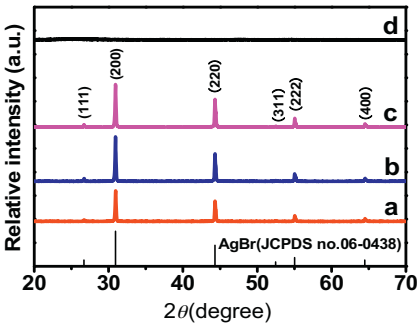

Fig. 3. XRD patterns of various samples: (a) AgBr; (b) Ti(IV)/AgBr (0.05 wt%); (c) Ti(IV)/AgBr (0.5 wt%); and (d) amorphous TiO_2 prepared from $Ti(SO_4)_2$ hydrolysis at 80 °C.

that of TiO_2. It is well known that the crystalline TiO_2 phase could be formed at a calcination temperature higher than 400 °C [38] or a hydrothermal temperature over 100 °C [39,40]. Considering a low-temperature modification progress (80 °C) in this study, the Ti(IV) compounds may be ascribed to amorphous $TiO(OH)_2$ or TiO_2 phase in the Ti(IV)/AgBr photocatalyst (Fig. 3c). In fact, the amorphous Ti(IV) can be further demonstrated by the low-temperature hydrolysis of $Ti(SO_4)_2$ under an identical synthetic method as the Ti(IV)/AgBr (Fig. 3d). Therefore, it is believed that the amorphous Ti(IV) cocatalyst has successfully been loaded on the AgBr surface.

XPS, a surface analysis technique, can further be used to demonstrate the successful loading of amorphous Ti(IV) on the AgBr surface. Fig. 4A shows the XPS survey spectra of different samples. It can be seen that before and after loading Ti(IV) cocatalyst, all

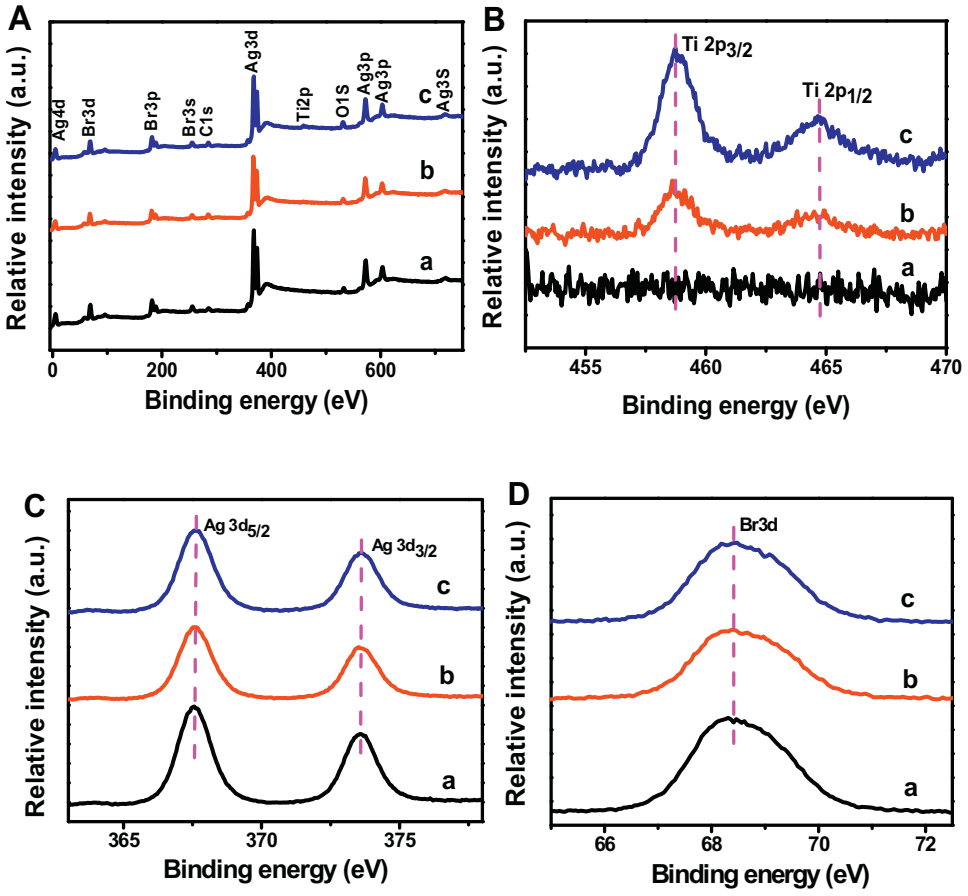

Fig. 4. (A) XPS survey spectra and the high-resolution XPS spectra of (B) Ti 2p, (C) Ag 3d, and (D) Br 3d for various samples: (a) AgBr; (b) Ti(IV)/AgBr (0.05 wt%); and (c) Ti(IV)/AgBr (0.5 wt%).

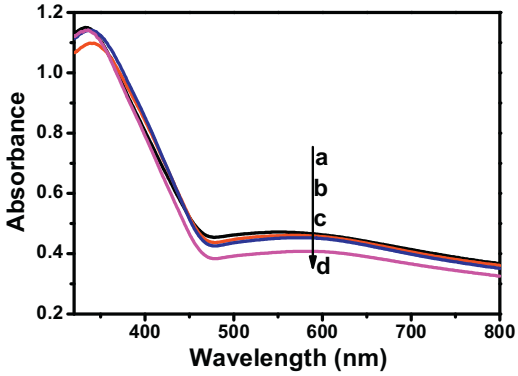

Fig. 5. UV–vis spectra of various samples: (a) AgBr; (b) Ti(IV)/AgBr (0.01 wt%); (c) Ti(IV)/AgBr (0.05 wt%); and (d) Ti(IV)/AgBr (0.5 wt%).

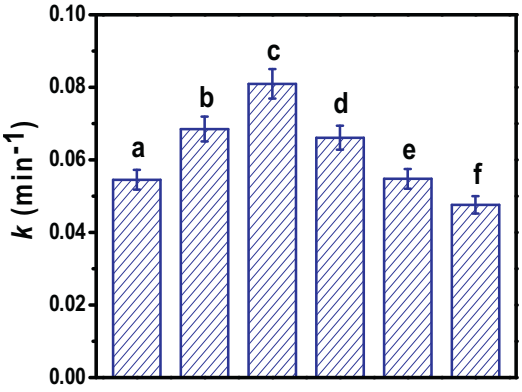

Fig. 6. The decomposition rate constant (k) of phenol solution by various photocatalysts: (a) AgBr; (b) Ti(IV)/AgBr (0.01 wt%); (c) Ti(IV)/AgBr (0.05 wt%); (d) Ti(IV)/AgBr (0.1 wt%); (e) Ti(IV)/AgBr (0.5 wt%); and (f) Ti(IV)/AgBr (1 wt%).

samples contain the main binding-energy peaks of Ag, Br, C, and O elements. The Ag and Br elements come from AgBr powders, and the C element is mainly caused by the carbon source from XPS instrument, while the O element is possibly from the adsorbed water during sample preparation or amorphous Ti(IV) compounds. Compared with pure AgBr (Fig. 4A-a), Ti(IV)/AgBr (0.05 wt%) shows no obvious binding energy peak of Ti element owing to the extremely small amount of Ti(IV) cocatalyst (Fig. 4A-b). However, when the amount of Ti(IV) is increased to 0.5 wt%, a new peak belonging to Ti element can be observed in the Ti(IV)/AgBr photocatalyst (Fig. 4A-c). To further reveal the Ti element and its chemical state, the high-resolution XPS spectra of the above samples are shown in Fig. 4B. Compared with the pure AgBr (Fig. 4B-a), the Ti(IV)/AgBr (0.05 wt%) (Fig. 4B-b) shows the obvious XPS peaks of Ti element. The binding energies of Ti $2p_{3/2}$ and Ti $2p_{1/2}$ are located at 458.7 and 464.7 eV, respectively, suggesting that the Ti cocatalyst is in the 4+ state [41]. The Ti(IV)/AgBr (0.5 wt%) (Fig. 4B-c) shows the similar Ti 2p XPS peaks as Ti(IV)/AgBr (0.05 wt%). However, their intensity of Ti $2p_{3/2}$ and Ti $2p_{1/2}$ peaks is clearly stronger than that of Ti(IV)/AgBr (0.05 wt%) owing to a larger amount of Ti(IV) cocatalyst. In addition, the binding energy position of Ti element in Ti(IV)/AgBr (0.05 wt%) (Fig. 4B-b) and Ti(IV)/AgBr (0.5 wt%) (Fig. 4B-c) shows no shift, indicating that the loaded Ti species maintain its 4+ state with the increasing content of Ti(IV) cocatalyst. Fig. 4C and D shows the Ag 3d and Br 3d XPS results, respectively. The binding energies of Ag $3d_{5/2}$ and $3d_{3/2}$ are located at 367.6 eV and 373.6 eV, respectively, which can be mainly attributed to the Ag^+ ion in AgBr [12], and the Br 3d at 68.5 eV can be mainly attributed to the Br^- ion in AgBr. It is found that the peak intensity and position show no shift, indicating that the loading of Ti(IV) cocatalyst cannot significantly influence the surface structure of AgBr photocatalyst. According to the element component analysis based on the XPS results, it is clear that the contents of Ti(IV) cocatalyst in the Ti(IV)/AgBr (0.05 wt%) and Ti(IV)/AgBr (0.5 wt%) are 2.16 at% and 4.29 at%, respectively. The above results further confirm that the Ti(IV) cocatalyst has been successfully modified on the AgBr surface.

The UV–vis spectra of AgBr and Ti(IV)/AgBr photocatalysts are shown in Fig. 5. It is obvious that the pure AgBr (Fig. 5a) exhibits a strong visible light absorption in the range of 470–800 nm in addition to its band gap absorption (ca. 470 nm). The wide visible-light absorption of AgBr particles can be attributed to the localized surface plasmon resonance (LSPR) effect of metallic Ag nanoparticles on the AgBr surface. After surface modification by Ti(IV) cocatalyst, the resultant Ti(IV)/AgBr photocatalysts present a similar absorption curve owing to its very limited amount of Ti(IV) cocatalyst on the AgBr surface. Therefore, it is very clear that the visible-light absorption of AgBr particles could be well maintained after coupling with Ti(IV) cocatalyst.

3.2. Photocatalytic activity and mechanism of Ti(IV)/Ag-based photocatalysts

The photocatalytic performance of the AgBr and Ti(IV)/AgBr photocatalysts are evaluated via the photodegradation of phenol solution under visible-light irradiation. As shown in Fig. 6, the individual AgBr photocatalyst (Fig. 6a) displays a comparable photocatalytic activity, and the k value is about 0.054 min^{-1}. After modification by Ti(IV) cocatalyst, the visible-light activities of Ti(IV)/AgBr photocatalysts firstly increase and then reach the maximum value when Ti(IV) cocatalyst is 0.05 wt%. The corresponding photocatalytic rate constant of Ti(IV)/AgBr (0.05 wt%) is 0.081 min^{-1}, which is higher than that of bare AgBr by a factor of 1.5. However, the photocatalytic performance of Ti(IV)/AgBr photocatalysts decreases when the content of Ti(IV) cocatalyst further increases. This phenomenon is in good agreement with the widely reported cocatalyst-modified photocatalysts such as Ag/AgCl–rGO [42] and Cu(II)/AgCl [28].

Since the Ti(IV) cocatalyst can effectively improve the photocatalytic activity of AgBr, it is very interesting and necessary to examine whether it can serve as a general cocatalyst to enhance the photocatalytic performance of other Ag-based photocatalysts. In addition to AgBr, we also prepared AgCl, AgI, Ag_2O, Ag_2CO_3, and Ag_3PO_4 materials by a simple precipitation method, and the loading of Ti(IV) cocatalyst was the same as that of Ti(IV)/AgBr samples. The resulting photocatalytic results are shown in Fig. 7A. It is clear that all the Ti(IV)/Ag-based photocatalysts show a higher photocatalytic performance than the corresponding unmodified Ag-based samples. Among them, the Ag_2O photocatalyst exhibits the best photocatalytic performance. Therefore, the above results strongly prove that Ti(IV) cocatalyst can be used as an effective and general hole cocatalyst to enhance the photocatalytic performance of Ag-based photocatalysts.

It is well known that the crystalline TiO_2 (rutile, brookite and anatase) is an excellent photocatalytic material for water splitting and organic substance degradation, while the amorphous TiO_2 shows no photocatalytic activity [43]. Compared with the crystalline TiO_2, amorphous Ti(IV) shows an obviously different microstructures, which can possibly produce some new important applications. Recently, amorphous Ti(IV) has been demonstrated to be an effective hole cocatalyst to improve the photocatalytic performance of rutile TiO_2 [35]. Thus, in the present study, it is believed that the amorphous Ti(IV) can also work as a hole cocatalyst to enhance the photocatalytic performance of Ag-based photocatalysts. Fig. 7B shows the possible photocatalytic mechanism of Ti(IV)-modified Ag-based photocatalysts. Under the visible-light irradiation, the photogenerated electrons and holes can be pro-

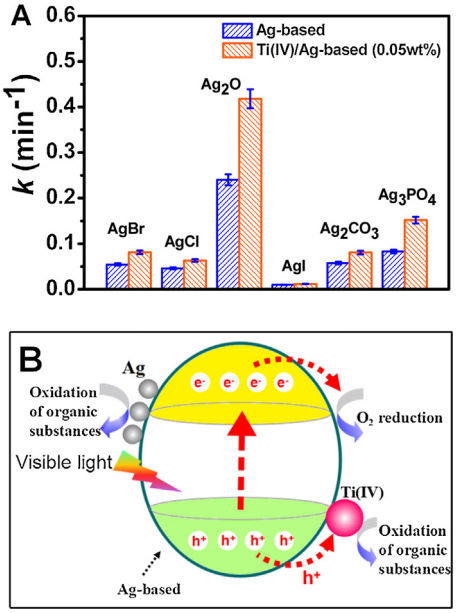

Fig. 7. (A) Photocatalytic performance of various Ag-based photocatalysts for the photodegradation of phenol; (B) The possible photocatalytic mechanism of Ti(IV)/Ag-based photocatalysts.

duced by the bandgap excitation of Ag-based photocatalysts or LSPR of Ag nanoparticles. In this case, Ti(IV) cocatalyst, as a hole-capture center, can trap the photogenerated holes from the VB of Ag-based materials, which is beneficial for the rapid separation of photogenerated charges and the following effective oxidization of organic substances. Therefore, the photocatalytic performance of Ag-based photocatalysts can be clearly improved by the surface loading of Ti(IV) hole cocatalyst.

3.3. Enhanced photoinduced stability of Ti(IV)/AgBr by loading of Fe(III) cocatalyst

As for an excellent photocatalytic material, possessing a stable photocatalytic performance is very important. To further investigate the performance stability of the Ti(IV)/AgBr (0.05 wt%) photocatalyst, we carried out five-cycle photocatalytic experiments for phenol decomposition, and the corresponding results are shown in Fig. 8. It is found that compared with the AgBr photocatalyst, the Ti(IV)/AgBr (0.05 wt%) photocatalyst shows a higher photocatalytic activity for its first cycle. However, after one-cycle of photocatalytic experiment, the Ti(IV)/AgBr (0.05 wt%) photocatalyst shows a gradually decreased photocatalytic performance during the remaining four cycles. Especially, in the fifth cycle, the

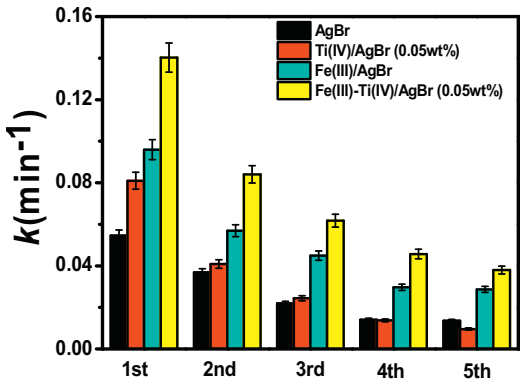

Fig. 8. Cycling runs of various samples for the photodegradation of phenol.

Ti(IV)/AgBr (0.05 wt%) photocatalyst exhibits a lower photocatalytic performance than the unmodified AgBr.

To account for the instable performance of Ti(IV)/AgBr (0.05 wt%), a possible mechanism is proposed (Fig. 9a and b). When the AgBr photocatalyst is illuminated by visible light, the photogenerated electrons are produced on the CB of AgBr particles while photogenerated holes remain in its valence band (VB). The photogenerated electrons can be used to reduce oxygen (route (1) in Fig. 9a), and the photogenerated holes are used to decompose organic materials such as phenol (Fig. 9a). After surface modification of AgBr by Ti(IV) hole cocatalyst (Fig. 9b), the photogenerated holes in the VB of AgBr particles tend to transfer to the Ti(IV) active sites to oxidize organic pollutants. As a consequence, the Ti(IV)/AgBr (0.05 wt%) exhibits a higher photocatalytic performance for the degradation of organic substances. However, owing to the rapid capture of photogenerated holes by Ti(IV) cocatalyst, more photogenerated electrons are accumulated on the CB of AgBr, which can lead to the reduction of more surface Ag^+ ions (route (2) in Fig. 9b). In fact, the formation of more metallic Ag can be well demonstrated by their XRD results, as shown in Fig. 10. It is found that compared with the bare AgBr (Fig. 10a), the Ti(IV)/AgBr sample (Fig. 10b) clearly shows a stronger diffraction peak of Ag phase after three-cycle photodegradation of phenol solution. Therefore, it can be suggested that the formation of more metallic Ag phase in AgBr photocatalyst causes an obvious deactivation process (as shown in Fig. 8), in good agreement with our previous studies [20,23]. The above results illustrate that the loading of Ti(IV) cocatalyst could result in a quick deactivation rate of AgBr particles. As a consequence, it is very meaningful and important to develop effective strategies to suppress the deactivation rate and enhance the performance stability of Ti(IV)/AgBr photocatalyst.

On the basis of above results, to efficiently suppress the deactivation of AgBr, it is quite necessary to promote the rapid capture of photogenerated electrons from the AgBr surface. In our previous

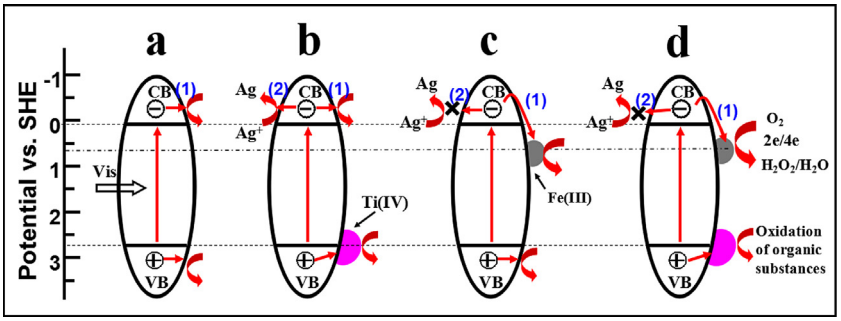

Fig. 9. Schematic diagrams illustrating the possible photocatalytic mechanism: (a) AgBr; (b) Ti(IV)/AgBr (0.05 wt%); (c) Fe(III)/AgBr; and (d) Fe(III)–Ti(IV)/AgBr (0.05 wt%). Route (1) represents the oxygen reduction reaction by photogenerated electrons, while Route (2) represents the reduction reaction of surface lattice Ag^+ to metallic Ag.

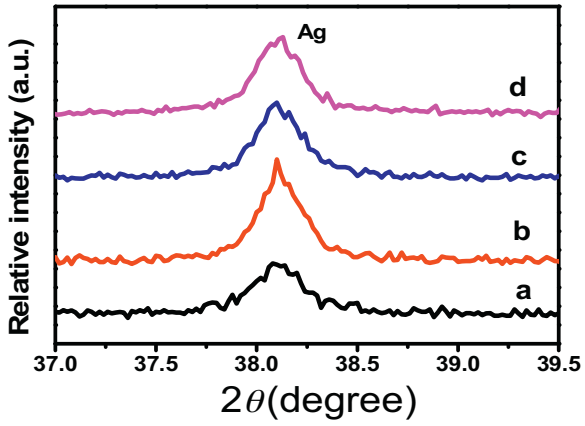

Fig. 10. The diffraction peaks of metallic Ag for various samples after third-cycle photocatalytic test: (a) AgBr; (b) Ti(IV)/AgBr (0.05 wt%); (c) Fe(III)/AgBr; and (d) Fe(III)–Ti(IV)/AgBr (0.05 wt%).

study, amorphous Fe(III) was demonstrated to be an efficient electron cocatalyst to quickly capture the photogenerated electrons, which can effectively inhibit the reduction of surface lattice Ag^+ in AgBr [12]. To suppress the deactivation of Ti(IV)/AgBr and to further enhance its photocatalytic performance, Fe(III) electron-cocatalyst was also loaded on its surface to prepare Fe(III)–Ti(IV)/AgBr by a facile impregnation method (Fig. 1d). For comparison, we also prepared Fe(III)/AgBr photocatalyst under an identical condition (Fig. 1b). According to the five-cycle experimental results (Fig. 8), it is clear that the Fe(III)/AgBr photocatalysts exhibit a higher photocatalytic performance than bare AgBr during repeating tests, which is in good agreement with our previous research [12]. After the Fe(III) cocatalyst is further coated on the Ti(IV)/AgBr surface, the resulting Fe(III)–Ti(IV)/AgBr (0.05 wt%) photocatalyst shows the highest photocatalytic activity. In fact, the completely photocatalytic decomposition of phenol solution can be well demonstrated by the UV–vis spectra (Fig. S1), where the concentration of phenol clearly decreases with increasing irradiation time. Even after five times of photocatalytic tests, the Fe(III)–Ti(IV)/AgBr (0.05 wt%) photocatalyst still shows a higher photocatalytic activity (0.038 min^{-1}) than the pure AgBr (0.013 min^{-1}) by a factor of 2.9, suggesting that the loading of Fe(III) cocatalyst not only can maintain the excellent photoinduced stability of Ti(IV)/AgBr (0.05 wt%) photocatalyst, but also can significantly enhance its photocatalytic activity. To further investigate its photoinduced stability, the Fe(III)–Ti(IV)/AgBr samples before and after repeated photocatalytic reactions are tested by XPS and their corresponding results are shown in Fig. S2. It is clear that after repeated photocatalytic reactions, the resultant Fe(III)–Ti(IV)/AgBr (0.05 wt%) still exhibits a similar binding energy for various elements such as Ti(IV), Fe(III) and Ag (a low-intensity XPS peaks for various elements are mainly caused by the accumulation of C element during the decomposition of organic substances), strongly suggesting the stable structure of Fe(III)–Ti(IV)/AgBr photocatalysts.

In view of the above results, it is very meaningful to investigate the possible photocatalytic mechanism of Fe(III)–Ti(IV)/AgBr (0.05 wt%) photocatalyst (Fig. 9c and d). For the Fe(III)/AgBr (Fig. 9c), its photocatalytic mechanism is completely different from that of the Ti(IV)/AgBr (0.05 wt%) photocatalyst (Fig. 9b). According to our previous results [12], the photogenerated electrons in the CB of AgBr are preferably transferred to oxygen via the Fe(III) electron-cocatalyst, causing an effective oxidization of phenol by the photogenerated holes on the VB of AgBr, showing a higher photocatalytic performance than the bare AgBr. Considering the rapid transfer of surface photogenerated electrons by the Fe(III) cocatalyst, it is clear that the metallic Ag in Fe(III)/AgBr (Fig. 10c) shows a lower amount than the Ti(IV)/AgBr (0.05 wt%) (Fig. 10b). When both of Fe(III) and Ti(IV) cocatalysts are simultaneously modified on the AgBr surface (Fig. 9d), the Ti(IV) cocatalyst can serve as a hole-capture center to rapidly capture photoinduced holes to oxidize organic pollutants, while the Fe(III) cocatalyst can be used as the oxygen-reduction active site to effectively inhibit the reduction of surface lattice Ag^+ (Fig. 10d). Owing to the synergistic action of Fe(III) and Ti(IV) cocatalysts, the resultant Fe(III)–Ti(IV)/AgBr (0.05 wt%) photocatalyst exhibits an obviously enhanced photoinduced stability and photocatalytic activity (Fig. 8).

For an efficient photocatalyst, the simultaneously rapid transfer of photogenerated charges from photocatalyst to the reaction active sites and their induced interfacial redox reactions are highly required. For a single-cocatalyst modified photocatalysts such as Fe(III)/AgBr and Ti(IV)/AgBr, their photocatalytic performance usually shows a relatively limited improvement considering their lack of oxidation or reduction active sites. Obviously, the simultaneous loading of a photocatalyst by electron and hole cocatalysts is a quite effective strategy to obtain the highest photocatalytic performance (in this case, Fe(III)–Ti(IV)/AgBr). However, most of the widely reported electron or hole cocatalysts are noble metals (Pt and Au as electron cocatalyst [44,45]) or their oxides (Ru_2O and IrO_2 as hole cocatalysts [29,30]). Therefore, it is very necessary to develop low-cost and earth-abundant materials as the high-performance cocatalyst for the further improvement of photocatalytic efficiency. In this study, considering the large amount of Ti and Fe elements in natural resources and their nontoxic properties, the present Ti(IV) and Fe(III) cocatalysts are possible to be widely applied in various photocatalytic materials to improve their photocatalytic performance.

4. Conclusions

In summary, Ti(IV) was first demonstrated be an effective and general hole cocatalyst to significantly improve the photocatalytic performance of various Ag-based photocatalysts such as AgCl, AgBr, AgI, Ag_2O, Ag_2CO_3, and Ag_3PO_4. However, owing to the rapid transfer of photogenerated holes by Ti(IV) cocatalyst, more photogenerated electrons were accumulated on the CB of AgBr, causing an obvious deactivation due to the reduction of surface lattice Ag^+ ions to metallic Ag. After the further surface loading by Fe(III) electron-cocatalyst, it was found that the photoinduced stability and photocatalytic activity of Ti(IV)/AgBr were significantly enhanced. The possible reason is due to the synergistic action of amorphous Ti(IV) and Fe(III) cocatalysts, namely, Ti(IV) cocatalyst acts as a hole-capture center to efficiently transfer holes to oxidize organic contaminants, while Fe(III) cocatalyst functions as a reduction active site to reduce oxygen efficiently. The present work opens a new sight for the development of highly efficient photocatalysts for the degradation of organic pollutants.

Acknowledgements

This work was supported by the National Natural Science Foundation of China (51472192, 21277107, 21477094, and 61274129) and 973 Program (2013CB632402). This work was also financially supported by program for new century excellent talents in university (NCET-13-0944), Wuhan Youth Chenguang Program of Science and Technology (2014070404010207), and the Fundamental Research Funds for the Central Universities (WUT 2015IB002).

Appendix A. Supplementary data

Supplementary data associated with this article can be found, in the online version, at http://dx.doi.org/10.1016/j.apcatb.2016.01.011.

References

[1] C.C. Chen, W.H. Ma, J.C. Zhao, Chem. Soc. Rev. 39 (2010) 4206–4219.
[2] Q.J. Xiang, B. Cheng, J.G. Yu, Angew. Chem. Int. Ed. 54 (2015) 11350–11366.
[3] G. Yin, M. Nishikawa, Y. Nosaka, N. Srinivasan, D. Atarashi, E. Sakai, M. Miyauchi, ACS Nano 9 (2015) 2111–2119.
[4] S. Wang, L. Pan, J.-J. Song, W. Mi, J.-J. Zou, L. Wang, X. Zhang, J. Am. Chem. Soc. 137 (2015) 2975–2983.
[5] R. Asahi, T. Morikawa, H. Irie, T. Ohwaki, Chem. Rev. 114 (2014) 9824–9852.
[6] W. Ho, Z. Zhang, M. Xu, X. Zhang, X. Wang, Y. Huang, Appl. Catal. B: Environ. 179 (2015) 106–112.
[7] C. Han, L. Ge, C. Chen, Y. Li, Z. Zhao, X. Xiao, Z. Li, J. Zhang, J. Mater. Chem. A 2 (2014) 12594.
[8] J.G. Yu, G.P. Dai, B.B. Huang, J. Phys. Chem. C 113 (2009) 16394–16401.
[9] G.Q. Luo, X.J. Jiang, M.J. Li, Q. Shen, L.M. Zhang, H.G. Yu, ACS Appl. Mater. Interfaces 5 (2013) 2161–2168.
[10] P. Wang, B.B. Huang, X.Y. Qin, X.Y. Zhang, Y. Dai, J.Y. Wei, M.H. Whangbo, Angew. Chem. Int. Ed. 47 (2008) 7931–7933.
[11] P. Wang, B.B. Huang, X.Y. Zhang, X.Y. Qin, H. Jin, Y. Dai, Z.Y. Wang, J.Y. Wei, J. Zhan, S.Y. Wang, J.P. Wang, M.H. Whangbo, Chem.-A Eur. J. 15 (2009) 1821–1824.
[12] H. Yu, L. Xu, P. Wang, X. Wang, J. Yu, Appl. Catal. B: Environ. 144 (2014) 75–82.
[13] P. Wang, B.B. Huang, Q.Q. Zhang, X.Y. Zhang, X.Y. Qin, Y. Dai, J. Zhan, J.X. Yu, H.X. Liu, Z.Z. Lou, Chem.-A Eur. J. 16 (2010) 10042–10047.
[14] C. Hu, T.W. Peng, X.X. Hu, Y.L. Nie, X.F. Zhou, J.H. Qu, H. He, J. Am. Chem. Soc. 132 (2010) 857–862.
[15] H. Yu, L. Liu, X. Wang, P. Wang, J. Yu, Y. Wang, Dalton Trans. 41 (2012) 10405–10411.
[16] Z. Yi, J. Ye, N. Kikugawa, T. Kako, S. Ouyang, H. Stuart-Williams, H. Yang, J. Cao, W. Luo, Z. Li, Y. Liu, R.L. Withers, Nat. Mater. 9 (2010) 559–564.
[17] H. Yu, G. Cao, F. Chen, X. Wang, J. Yu, M. Lei, Appl. Catal. B: Environ. 160–161 (2014) 658–665.
[18] X. Yang, H. Cui, Y. Li, J. Qin, R. Zhang, H. Tang, ACS Catal. 3 (2013) 363–369.
[19] Y.P. Bi, S.X. Ouyang, J.Y. Cao, J.H. Ye, Phys. Chem. Chem. Phys. 13 (2011) 10071–10075.
[20] X.F. Wang, S.F. Li, H.G. Yu, J.G. Yu, S.W. Liu, Chem.-A Eur. J. 17 (2011) 7777–7780.
[21] H.G. Yu, R. Liu, X.F. Wang, P. Wang, J.G. Yu, Appl. Catal. B: Environ. 111 (2012) 326–333.
[22] X. Wang, S. Li, H. Yu, J. Yu, J. Mol. Catal. A: Chem. 334 (2011) 52–59.
[23] X. Wang, S. Li, Y. Ma, H. Yu, J. Yu, J. Phys. Chem. C 115 (2011) 14648–14655.
[24] S. Lou, X. Jia, Y. Wang, S. Zhou, Appl. Catal. B: Environ. 176–177 (2015) 586–593.
[25] X. Wang, C. Fu, P. Wang, H. Yu, J. Yu, Nanotechnology 24 (2013) 165602.
[26] F.-M. Zhao, L. Pan, S. Wang, Q. Deng, J.-J. Zou, L. Wang, X. Zhang, Appl. Surf. Sci. 317 (2014) 833–838.
[27] J.G. McEvoy, Z.S. Zhang, Appl. Catal. B: Environ. 160 (2014) 267–278.
[28] P. Wang, Y. Xia, P. Wu, X. Wang, H. Yu, J. Yu, J. Phys. Chem. C 118 (2014) 8891–8898.
[29] T. Ohno, L. Bai, T. Hisatomi, K. Maeda, K. Domen, J. Am. Chem. Soc. 134 (2012) 8254–8259.
[30] M. Higashi, K. Domen, R. Abe, Energy Environ. Sci. 4 (2011) 4138.
[31] J. Yang, H. Yan, X. Wang, F. Wen, Z. Wang, D. Fan, J. Shi, C. Li, J. Catal. 290 (2012) 151–157.
[32] M. Higashi, K. Domen, R. Abe, J. Am. Chem. Soc. 134 (2012) 6968–6971.
[33] M.H. Pham, C.T. Dinh, G.T. Vuong, N.D. Ta, T.O. Do, Phys. Chem. Chem. Phys. 16 (2014) 5937–5941.
[34] Y.P. Xie, G. Liu, G.Q. Lu, H.M. Cheng, Nanoscale 4 (2012) 1267–1270.
[35] M. Liu, R. Inde, M. Nishikawa, X. Qiu, D. Atarashi, E. Sakai, Y. Nosaka, K. Hashimoto, M. Miyauchi, ACS Nano 8 (2014) 7229–7238.
[36] D. Eisenberg, H.S. Ahn, A.J. Bard, J. Am. Chem. Soc. 136 (2014) 14011–14014.
[37] S. Hu, M.R. Shaner, J.A. Beardslee, M. Lichterman, B.S. Brunschwig, N.S. Lewis, Science 344 (2014) 1005–1009.
[38] C.H. Heo, S.-B. Lee, J.-H. Boo, Thin Solid Films 475 (2005) 183–188.
[39] J.-N. Nian, H. Teng, J. Phys. Chem. B 110 (2006) 4193–4198.
[40] J. Zhang, X. Xiao, J. Nan, J. Hazard. Mater. 176 (2010) 617–622.
[41] J. Singh, A. Gusain, V. Saxena, A.K. Chauhan, P. Veerender, S.P. Koiry, P. Jha, A. Jain, D.K. Aswal, S.K. Gupta, J. Phys. Chem. C 117 (2013) 21096–21104.
[42] P. Wang, T. Ming, G. Wang, X. Wang, H. Yu, J. Yu, J. Mol. Catal. A: Chem. 381 (2014) 114–119.
[43] C. Damm, D. Völtzke, H.P. Abicht, G. Israel, J. Photochem. Photobiol. A: Chem. 174 (2005) 171–179.
[44] J.-J. Zou, H. He, L. Cui, H.-Y. Du, Int. J. Hydrogen Energy 32 (2007) 1762–1770.
[45] T. Yan, H. Zhang, Y. Liu, W. Guan, J. Long, W. Li, J. You, RSC Adv. 4 (2014) 37220–37230.